Renewable Energy 200 (2022) 1008–1022

Contents lists available at ScienceDirect

Renewable Energy

journal homepage: www.elsevier.com/locate/renene

Paving the way towards an eco- and budget-friendly one-pot catalytic conversion of cellulose and lignocellulosic residues into ethylene glycol over Ni–W/CNT catalysts

Lucília Sousa Ribeiro [a,b,*], Ana Luzia Ferreira Pires [a,b], José Joaquim de Melo Órfão [a,b], Manuel Fernando Ribeiro Pereira [a,b]

[a] LSRE-LCM - Laboratory of Separation and Reaction Engineering – Laboratory of Catalysis and Materials, Faculty of Engineering, University of Porto, Rua Dr. Roberto Frias, 4200-465, Porto, Portugal

[b] ALiCE - Associate Laboratory in Chemical Engineering, Faculty of Engineering, University of Porto, Rua Dr. Roberto Frias, 4200-465, Porto, Portugal

ARTICLE INFO

Keywords:
Biomass wastes
Cellulose
Ni–W/CNT catalysts
Hydrolytic hydrogenation
Ethylene glycol

ABSTRACT

The increasing demand for ethylene glycol (EG) for the manufacture of polyester fibers and resins in the plastic industry and as antifreeze in the automotive industry, together with the urge to replace fossil resources by renewable alternatives, leads today's society for the search of new sustainable processes like EG production from biomass. However, although many studies have been conducted on the catalytic conversion of cellulose to EG, the main issue that remains a challenge is to achieve adequate catalyst stability. To fulfil this gap, herein, a series of Ni–W-based catalysts supported on carbon nanotubes (CNT) were prepared and characterized by several techniques (TG, SEM, EDS, XRD, ICP and N_2 adsorption). Cellulose was initially used as model feedstock for a comparative study on its reaction pathways, which effective control is fundamental to maximize EG production. In this work, cellulose was completely converted over Ni–W/CNT catalysts producing an EG yield over 50% after 5 h. The notable performance was attributed to the equilibrium between retro-aldol condensation and hydrogenation reactions achieved through the optimal conjugation of nickel and tungsten active sites. The best catalyst was then evaluated for EG direct production from lignocellulosic residues, such as eucalyptus wood, corncob and cotton wool. Unprecedented EG yields up to 46% were directly attained from the lignocellulosic wastes in just cheap and non-toxic water in the presence of pressurized hydrogen, under mild conditions and using promising environmentally friendly and cost-effective earth-abundant metal catalysts in replacement of noble metals (e.g. Ru). The catalysts presented good stability in hydrothermal conditions during repeated use for at least 6 cycles, demonstrating a promising outlook for future developments. Accordingly, 20%Ni–20%W/CNT is here presented as a potential cost-effective catalyst solution for the mandatory reduction of the dependence on petroleum.

1. Introduction

The reliance on fossil fuel reserves and other non-renewable sources has a massive impact on the global environment. One of the most important advances in green chemistry stimulated by industry is the conversion of lignocellulosic biomass to value-added products and fuels [1,2]. Lignocellulosic biomass, as raw material, has shown a great potential since it is renewable, abundant and easily accessed worldwide [3,4]. It is mainly composed of cellulose, hemicelluloses and lignin, but due to its highly crystalline structure and high resistance to chemical transformations, lignocellulosic biomass conversion is a challenging task and usually requires adequate pre-treatments [5–7]. One of the most interesting routes for biomass valorisation is its hydrolytic hydrogenation into added value products, such as ethylene glycol (EG) that is still dependent on petroleum and the cracking process [1,8]. This product has a large market demand for the development of pharmaceuticals and cosmetics, and is widely used for manufacturing polyesters and resins in the plastics industry and as antifreeze in automotive industries [9,10].

The one-pot biomass conversion process to EG can be summed up in three steps: firstly, hydrolysis to sugar monomers (e.g. glucose, xylose), promoted by protons from hot water or from acidic environment; then,

* Corresponding author. LSRE-LCM - Laboratory of Separation and Reaction Engineering – Laboratory of Catalysis and Materials, Faculty of Engineering, University of Porto, Rua Dr. Roberto Frias, 4200-465, Porto, Portugal.

E-mail addresses: lucilia@fe.up.pt (L.S. Ribeiro), 201905797@edu.fe.up.pt (A.L.F. Pires), jjmo@fe.up.pt (J.J.M. Órfão), fpereira@fe.up.pt (M.F.R. Pereira).

https://doi.org/10.1016/j.renene.2022.10.026
Received 16 May 2022; Received in revised form 4 October 2022; Accepted 6 October 2022
Available online 15 October 2022

Abbreviations

AC – activated carbon
BET – Brunauer-Emmett-Teller
BMC – ball-milled cellulose
BSED – backscattered electrons detector
CNT – carbon nanotubes
EDS – energy dispersive spectroscopy
EG – ethylene glycol
FA – formic acid
GA – glycolaldehyde
Gly – glycerol
HPLC – high performance liquid chromatography
ICP – inductively coupled plasma
IUPAC – International Union of Pure and Applied Chemistry
LA – levulinic acid
LFD – large field detector
MCC – microcrystalline cellulose
PG – propylene glycol (1,2-propanediol)
RAC – retro-aldol condensation
RI – refractive index
SEM – scanning electron microscopy
SOR – sorbitol
TG – thermogravimetric analysis
TOC – total organic carbon
TPR – temperature programmed reduction
XRD – X-ray diffraction

retro-aldol condensation (RAC) of glucose to glycolaldehyde (GA); and finally the hydrogenation of GA to EG (route 2 in Fig. 1) [10,11]. However, the conversion of cellulose might follow a diversity of other routes, such as isomerization, dehydration, decarbonisation, hydration, dehydrogenation, etc., which originates secondary products like sorbitol, mannitol and levulinic acid, depending on the catalyst used that will promote different reactional routes due to its unique characteristics (e.g. routes 1 and 3 in Fig. 1) [12,13]. It has been proved that tungstic species have high selectivity to enhance the RAC step because they promote the cleavage of the C–C bond of cellulose, while Ni or noble metals like Ru or Pt catalyse the hydrogenation step [14,15]. Accordingly, to promote EG production, W-based catalysts should be used in conjunction with hydrogenation catalysts or bifunctional catalysts containing both active phases. Yet, one of the current main challenges in cellulose transformation is to maintain the catalyst stability. Catalyst deactivation can take place through carbon/coke formation, metal sintering and/or metal leaching. The deposition of carbon/coke causes the blockage of the active sites and metal pores and the support, hindering reactants' accessibility and interactions that eventually reduce the catalyst activity. So, an efficient catalyst should be designed.

In terms of ethylene glycol production, a ground-breaking achievement was attained for the first time in 2008, using the catalyst 2% Ni–30%W_2C supported on activated carbon (AC) with a yield of 61% after 30 min at 245 °C [16]. This work demonstrated that the usage of tungsten-based catalysts boosts the selectivity towards EG, which originated huge attention from academia and industry [17]. Subsequently, extensive studies have explored new catalysts to optimize the catalytic performance [1–3,8–10,18–36]. Some of the best results attained for EG over tungsten-based catalysts supported on carbon materials are listed in Table 1. Some authors have obtained EG yields around 75% from microcrystalline cellulose [14,31–33]. For example, Zheng et al. found that bimetallic catalysts 5%Ni–25%W/SBA-15 and 5%Ru–25%W/AC promoted an increase of EG yield up to 75 and 62%, respectively [14]. However, 5%Ni–25%W/SBA-15 could not be reused due to the total collapse of the mesoporous structure of SBA-15. On the other hand, the 5%Ru–25%W/AC catalyst overcame this problem, but the yield of EG attained was lower. Therefore, carbon materials became interesting as supports since they are tolerant to hydrothermal conditions and to acid-base attack, consequently being extremely stable. Also, both their porous texture and surface chemistry can be modified by appropriate methodologies. In addition to the most commonly used activated carbon support, carbon nanotubes (CNT) and carbon nanofibers have also been investigated as catalytic supports [19,34,37]. Although presenting good stability up to 2–3 cycles, an abrupt decrease is observed in subsequent runs due to retention of reaction products that shield active sites.

To the best of our knowledge, the less drastic reaction conditions reported so far for the conversion of cellulose into EG were initially studied by Liu et al. that obtained a conversion of 62% and an EG yield of

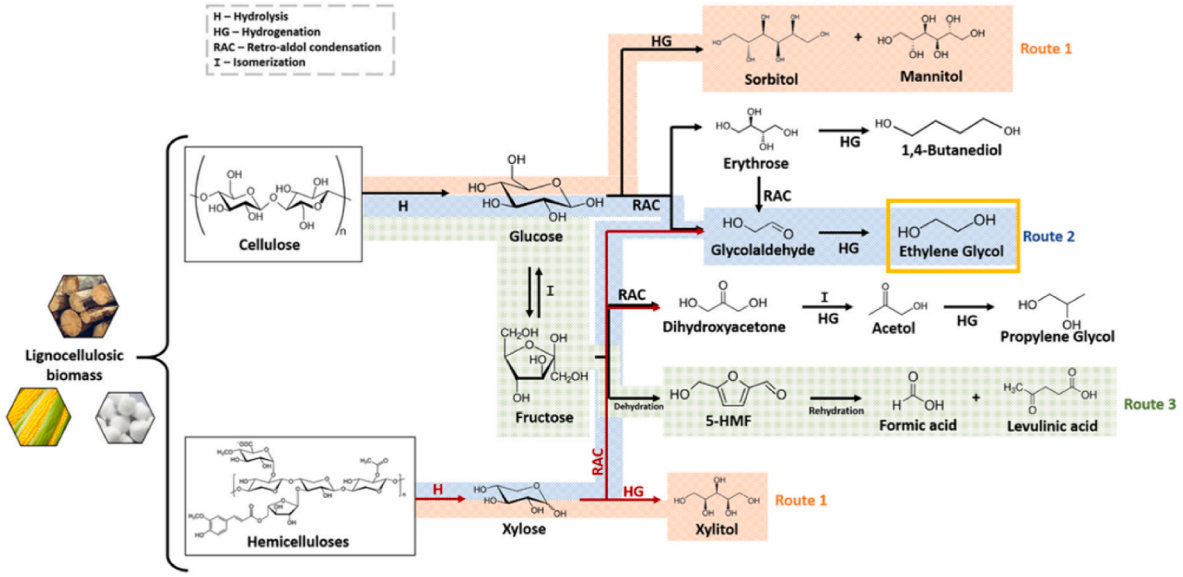

Fig. 1. Reaction pathways involved in biomass conversion to ethylene glycol.

Table 1
Results for cellulose conversion to EG over W-containing carbon-supported catalysts.

Catalyst	Substrate[a]	T (°C)	t (h)	P_{H2} (bar)	Conversion (%)	EG yield (%)	Ref.
3%Ru/C + 6%WO_3/C	MCC	205	0.5	60	62	35	[35]
0.8%Ru–30%W/CNT	BMC	205	3	50	100	40	[36]
0.4%Ru–30%W/CG_{HNO3}	BMC	205	5	50	100	42	[26]
0.4%Ru/CG_{HNO3} + 30%W/CG	BMC	205	5	50	100	48	[26]
15%Ni–20%W/CNT	MCC	240	2	50[b]	100	55	[34]
2%Ni–30%W_2C/AC	MCC	245	0.5	60[b]	100	61	[9,16]
5%Ru–25%W/AC	MCC	245	0.5	60[b]	100	62	[14]
2%Ni-30%WC_x/MC	MCC	245	0.5	60[b]	100	74	[31]
10%Ni–30%W_2C/AC	MCC	245	0.5	60[b]	100	73	[32]
2%Ni–20%WP/AC	MCC	245	0.5	60[b]	100	46	[3]
5%Ru–30%$W_{18}O_{40}$/graphene	MCC	245	1	60[b]	100	62	[29]
30%Cu-30%WO_x/AC + 10%Ni/AC	MCC	245	2	40[b]	100	70	[33]
5%Ru/AC + H_2WO_4	BMC	245	2	50[b]	100	58	[25]
20%Ni/AC + Sn powder	MCC	245	1.5	50[b]	100	58	[30]
30%NiWB/CNT	MCC	250	2	60[b]	100	58	[19]

[a] MCC and BMC are abbreviations for microcrystalline cellulose and ball-milled cellulose, respectively.
[b] Measured at room temperature.

35% at 205 °C and 60 bar of H_2 from microcrystalline cellulose in just 30 min [35]. Afterwards, our group was able to upgrade the EG yield to more than 40% after 5 h also at 205 °C, but from ball-milled cellulose (100% conversion), at 50 bar of H_2 and using a catalyst with only 0.4–0.8% of Ru [36]. Additionally, our group has reported bimetallic Ru–W catalysts supported on glucose-based carbons and carbon nanotubes for the direct production of EG from cellulose and lignocellulosic biomass wastes [13,26,36,38]. Although these recent works allowed to produce EG directly from cellulose and residues with reaction conditions significantly less drastic than the previously reported (e.g., 245 °C) and using a considerably lower content of noble Ru, there was still a dependency on this noble metallic phase. The excessive cost of noble metal-based catalysts is a significant obstacle. Therefore, the development of a less expensive but efficient catalyst to replace precious-metal catalysts is highly desirable, and non-noble metal nickel has been drawing lots of attention due to its low price. In fact, Ni-based catalysts exhibit impressive catalytic properties in many classic reactions like hydrogenation, making them valuable alternatives to conventional precious metals. Also, Ni-based catalysts are relatively stable compared to other metals such as Fe and Co, thus being promising for practical applications in industrial production. A series of Ni–W catalysts supported on various materials, including activated carbon [3,9,16,32,39], mesoporous carbon [31], TiO_2 [40], SiO_2 [15], Al_2O_3–SiO_2 [41] and SBA-15 [14,42], have been studied, but despite presenting good catalytic performance, they lack stability in order to be viable for industrial application. Furthermore, the resultant catalysts often have elevated specific surface energies and bind the doped active particles of the catalyst only via weak interaction, allowing the catalytic particles to easily migrate and agglomerate during reaction, which results in poor catalytic stability and decreased activity. To the best of our knowledge, the highest yields of EG obtained so far were around 73–74% over Ni–W catalysts supported on activated/mesoporous carbon (Table 1) [31,32]. However, these results were attained over relatively drastic reaction conditions of 245 °C and 60 bar of H_2 (at room temperature), and a significant loss of catalytic performance after just 3 recycling experiments. In fact, these groups observed that both Ni and W leached into the solution during reaction, which was considered to probably account for the deterioration of catalyst performance and consequent decrease in the yield of the main product. Accordingly, despite these high yields of EG achieved, the main issue of this process related to maintaining the catalyst stability still remains a challenge and lacks investigation.

Many advances were made for catalytic conversion of pure cellulose, but the conversion of raw lignocellulosic biomass is still an open issue and, herein, an efficient catalytic system is proposed. A promising and sustainable strategy for EG production directly from biomass includes using: i) hot water as solvent, which is a cheap non-toxic solvent and facilitates hydrolysis, ii) pre-treated (e.g., ball-milled) renewable substrates, and iii) bifunctional heterogeneous metal catalysts that catalyse not only hydrogenation but also RAC and hydrolysis and are easily recovered and reused. Furthermore, besides diminishing the environmental impact, replacing noble metals in the catalysts with cheaper earth-abundant transition metals (e.g., Mn, Fe, Co, Ni, Cu) or early transition metals (e.g., Ti, V, Cr, Zr, Nb, W) is also fundamental to bring down the catalyst cost. Thus, it is still necessary to optimize the reaction conditions and find a promising metallic phase capable of replacing noble metals. In the present work, we synthesized Ni–W catalysts and evaluated their catalytic performance and stability. Furthermore, the effect of the support and the optimal metal combination for cellulose conversion and EG production based on Ni–W bimetallic synergy was investigated. The prepared catalysts were submitted to less drastic and acid-free reaction conditions than most of the studies reported to date, with no use of noble metals as metallic phases.

2. Experimental

2.1. Chemicals and materials

Microcrystalline cellulose was purchased from Alfa Aesar, eucalytus wood (*Eucalyptus globulus*) and corncob were collected in the North region of Portugal, and cotton wool was bought locally. For the catalyst preparation, multiwalled carbon nanotubes (NANOCYL NC3100 series, with average diameter of 9.5 nm, average length of 1.5 μm and carbon purity higher than 95%), activated carbon GAC 1240 PLUS, nickel(II) nitrate hexahydrate ($Ni(NO_3)_2{\cdot}6H_2O$, 99.999%) and ammonium (meta) tungstate hydrate ($H_{26}N_6O_{41}W_{12}$.aq 99.999%, ≥85% WO_3) were supplied by Nanocyl, Norit, Sigma-Aldrich and Fluka, respectively. Sulphuric acid (>95%) was obtained from VWR. All solutions were prepared in ultrapure water (conductivity = 18.2 μS cm^{-1}) obtained in a Milli-Q Millipore system. Unless stated otherwise, all chemicals were used as received without any purification.

2.2. Pre-treatment of substrates

Eucalyptus wood and corncob were initially cut and crushed in appropriate apparatus and subsequently dried overnight in an oven at 100 °C, while cotton wool was used as purchased.

To reduce the substrate crystallinity, eucalyptus wood, corncob, cotton wool and cellulose were ball-milled for 4 h at a frequency of 20 s^{-1} prior to reaction, in a Retsch Mixer Mill MM200 equipped with two ceramic pots (10 mL), each one loaded with two ZrO_2 balls (12 mm of diameter).

2.3. Preparation of catalysts

A nickel and a tungsten monometallic catalysts (nominal metal loadings of 20 wt %) were prepared by the incipient wetness impregnation method of commercial carbon nanotubes (CNT) with a solution of $Ni(NO_3)_2{\cdot}6H_2O$ and $H_{26}N_6O_{41}W_{12}$.aq, respectively. The catalysts were denoted as 20%Ni/CNT and 20%W/CNT. Furthermore, following the same procedure, Ni–W bimetallic catalysts were prepared with different Ni loadings (1, 2, 5, 10, 20 and 30 wt %) and W loadings (5, 10, 20, 30 and 40 wt %). The synthesized catalysts were labelled as *x*%Ni-*y*%W/CNT, where *x* and *y* indicated the weight percentage of Ni and W, respectively. Typically, a 20%Ni–20%W/CNT catalyst was prepared by the incipient wetness impregnation method of commercial CNT with a solution of both Ni and W precursors. In addition, another catalyst loaded on activated carbon (AC) was prepared in the same way, and denoted as 20%Ni–20%W/AC.

After impregnation, the resulting samples were thermally treated for 3 h under N_2 flow (100 $cm^3\ min^{-1}$) and reduced for 3 h under H_2 flow (100 $cm^3\ min^{-1}$). The appropriate reduction temperatures (500 °C for Ni and Ni–W catalysts, and 700 °C for W catalyst) were determined by temperature programmed reduction (TPR) (see sections 2.4 and 3.1), and the thermal treatment occurred at the same temperature.

2.4. Physicochemical characterization

Cellulose, eucalyptus wood, corncob and cotton wool have been extensively characterized elsewhere [38,43], while the catalysts were examined by multiple analytic techniques as described below.

TPR was performed on an AMI 200 Altamira Instruments. The analyses were conducted on the fresh catalysts in a U-shaped quartz cell using a 5%H_2/He gas flow of 50 $cm^3\ min^{-1}$, with a heating rate of 10 °C min^{-1}.

N_2 physisorption was conducted on a Quantachrome NOVA 4200e equipment at −196 °C after the catalysts were degassed at 150 °C for 3 h. The specific surface area (S_{BET}) was calculated using the Brunauer-Emmett-Teller (BET) method. The total pore volume (V_p) was estimated by the single point N_2 adsorption at $P/P_0 = 0.99$. The micropores volume ($V_{\mu pores}$) and the external surface area (S_{ext}), considering all non-microporous surface, were determined by the t-method.

Thermogravimetric (TG) analysis was conducted on a STA 409 PC/4/H Luxx Netzsch thermal analyser. The catalyst was loaded in an Al_2O_3 crucible, and the temperature was programmed from 50 to 900 °C with a heating rate of 10 °C min^{-1} under inert (N_2, 99.999%) atmosphere. After reaching 900 °C, the catalyst was kept at this temperature for 7 min under N_2 followed by 13 min under air flow (99.999%) to burn off the carbon. The obtained results were used to determine the volatile matter, fixed carbon, and ash contents.

The quantification of nickel loading in the catalysts was performed by inductively coupled plasma (ICP) emission spectrometry. The analyses were carried out in a PerkinElmer Optima 4300 spectrometer using an optic with Echelle polychromator. The tungsten content was estimated from the difference between the total percentage of ashes in the metal supported catalysts (from TG) and the sum of Ni content (from ICP) with the ashes in the pristine support (from TG).

The powder X-ray diffraction (XRD) patterns of the catalysts were collected on a Philips X'Pert MPD diffractometer (Cu-Kα = 0.15406 nm). The diffracted intensity of Cu-Kα radiation was measured in the 2θ range between 10° and 100°.

Scanning electron microscopy (SEM) with energy dispersive X-ray spectroscopy (EDS) was applied to observe the morphology and metal dispersion of the catalysts. SEM/EDS images were taken on a high resolution (Schottky) Environmental Scanning Electron Microscope with X-Ray Microanalysis and Electron Backscattered Diffraction analysis: FEI Quanta 400 FEG ESEM/EDAX Genesis X4M. The catalysts, in powder form, were previously attached to an aluminium pin using conductive carbon double-sided adhesive tape. The analysis was conducted using a large field low vacuum detector (LFD) for secondary electrons and a backscattered electrons detector (BSED).

2.5. Catalytic reaction

The catalytic experiments were implemented in a 1000 mL stainless steel Parr reactor (USA Mod. 5120). In standard tests, 750 mg of ball-milled substrate (cellulose, eucalyptus, corncob, or cotton), 300 mg of catalyst and 300 mL of water were charged to the reactor under stirring at 300 rpm. Once loaded, the reactor was sealed, purged with N_2 (99.999%) for 5 min and subsequently pressurized to 5 bar. Afterwards, the reactor was placed into an electric heating jacket fitted with a temperature controller and heated to the desired temperature of 205 °C at a heating rate of approximately 2 °C min^{-1}. When the desired temperature was reached, the reaction was initiated by switching from inert gas to 50 bar of hydrogen (99.999%). At the end of the experiment (5 h), the reactor was removed from the heating jacket and cooled using a cooling fan, bringing the reactor temperature to ambient in 30 min with stirring. The catalyst was recovered by filtration, washed with deionized water, and dried overnight in an oven at 100 °C under air atmosphere to test the stability of the optimal catalyst. The collected reaction solution was analysed by atomic absorption spectroscopy (GBC 932 Plus) to test for metal(s) leaching to the solution.

Reproducibility tests were carried out in triplicate for the first catalytic tests and for key experiments (e.g., best catalytic system), followed by analysis of reaction products. The results from the analysis showed a standard deviation of less than 6 and 2% for conversions and yields, respectively, and so the remaining experiments were only undertaken once.

2.6. Product analysis

Representative samples were periodically withdrawn for analysis, without any pre-treatment other than filtration, centrifugation, and decantation. The centrifugation was performed in a VWR Microstar12 apparatus, during 5 min at a rotation speed of 13,500 rpm.

The aqueous products obtained were identified and quantified by high performance liquid chromatography (HPLC) using an Elite LaChrom HITACHI apparatus, equipped with a refractive index (RI) detector and an Alltech OA-1000 ion exclusion column (300 × 6.5 mm, mobile phase: 5 mmol min^{-1} of H_2SO_4 at 0.5 mL min^{-1}). The yield of each product was calculated as the ratio between the number of moles of carbon in the product formed (measured by HPLC) and the number of moles of carbon in the substrate initially present.

The conversion of cellulose and lignocellulosic substrates was determined based on total organic carbon (TOC) data, obtained with a TOC-L Shimadzu analyser. The conversion was calculated as the ratio between the number of moles of TOC in the resultant liquid and the number of moles of carbon in the substrate charged into the reactor. For the calculations, it was considered that cotton wool is only composed of cellulose and also that EG could only be produced from cellulose and hemicelluloses (holocellulose) in the cases of eucalyptus wood and corncob reactions.

3. Results and discussion

3.1. Characterization results

An extensive characterization was performed to investigate the properties of the different bifunctional catalysts prepared, and the obtained results are described as follows.

Fig. 2 shows the H_2-TPR profiles of mono- and bimetallic catalysts. The tungsten monometallic catalyst presented a peak between 700 and 820 °C due to the reduction of WO_x species, while the nickel monometallic catalyst profile showed two clearly defined peaks between 320 and 600 °C, suggesting the reduction of different oxidized species. As

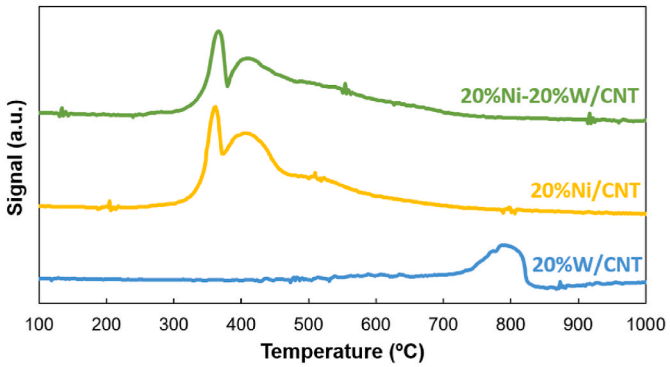

Fig. 2. TPR profiles of 20%Ni/CNT, 20%W/CNT and 20%Ni–20%W/CNT catalysts.

already explained by Wei et al. the hydrogen consumption peak around 350 °C may be assigned to the presence of reduced NiO species that interact moderately with carbon nanotubes, while the peak around 400 °C may be assigned to the reduction of NiO species that have a strong interaction with CNT [44]. The H_2-consumption profile of Ni–W bimetallic catalyst was similar to that of the Ni monometallic catalyst. Accordingly, to minimize metals sintering, reduction temperatures of 500 °C were selected for Ni and Ni–W catalysts, and 700 °C for W catalysts that was kept for 3 h.

The N_2 adsorption-desorption isotherms of the materials are plotted in Fig. 3. The CNT and the respective supported catalysts exhibited type-II adsorption curves accordingly to International Union of Pure and Applied Chemistry (IUPAC) classification, typical of non-microporous materials, unlike AC and 20%Ni–20%W/AC that mainly showed a microporous structure with partial mesoporosity. Pristine carbon nanotubes present a surface area of 267 $m^2\ g^{-1}$, most of its porosity corresponding to large mesopores that result from the free space in CNT bundles, while AC presents a much higher BET surface area (838 $m^2\ g^{-1}$) according to its well-developed micro-porosity (0.291 $cm^3\ g^{-1}$) (Table 2).

According to Table 2, the BET specific surface areas and pore volumes of the CNT supported catalysts were in the range of 121–232 $m^2\ g^{-1}$ and 0.432–1.378 $cm^3\ g^{-1}$, respectively. As expected, the surface area decreased with the introduction of the metal(s) phase(s) comparing to the pristine support, and the pore volume decreased accordingly, which can be attributed to a dilution effect resultant of the high loadings of nickel and/or tungsten. The surface areas of the metal loaded AC and CNT catalysts were reduced by a maximum of 46 and 54%, respectively, compared to that of the corresponding parent carbon (Table 2). Yet, the identical shapes of the N_2 isotherms of the parent AC and CNT comparing to those of the respective metal supported catalysts indicate that the texture of the carbon supports was not drastically changed during the catalyst preparation steps.

Table 2
Textural properties of the supports and catalysts.

Catalyst	S_{BET} ($m^2\ g^{-1}$)	S_{ext} ($m^2\ g^{-1}$)	$V_{\mu pores}$ ($cm^3\ g^{-1}$)	V_p ($cm^3\ g^{-1}$)
CNT	267	267	0.000	2.424
20%Ni/CNT	232	232	0.000	1.378
20%W/CNT	170	170	0.000	1.339
1%Ni–30%W/CNT	157	157	0.000	1.039
2%Ni–30%W/CNT	144	144	0.000	0.995
5%Ni–30%W/CNT	140	140	0.000	0.914
10%Ni–30%W/CNT	130	130	0.000	0.830
20%Ni–30%W/CNT	124	124	0.000	0.629
30%Ni–30%W/CNT	121	121	0.000	0.528
20%Ni–5%W/CNT	217	217	0.000	1.196
20%Ni–10%W/CNT	210	210	0.000	1.135
20%Ni–20%W/CNT	177	177	0.000	0.836
20%Ni–40%W/CNT	123	123	0.000	0.432
20%Ni–20%W/CNT used	176	176	0.000	0.904
AC	838	137	0.291	0.492
20%Ni–20%W/AC	455	90	0.154	0.288

The thermal decomposition course of the supports and metal-supported catalysts was verified by thermogravimetric analysis (TG). The proximate analysis was performed based on the thermal decomposition in inert and oxidizing atmospheres, allowing the determination of the content of volatiles, fixed carbon, and ashes (Table 3). As expected, a rise in the amount of ashes with the increase of metal loading in the catalyst was observed, roughly corresponding to the total content of metal(s) impregnated in the support.

The loading of nickel was determined by ICP. According to Table 4, the ICP results showed that the nickel loading was, in general, slightly

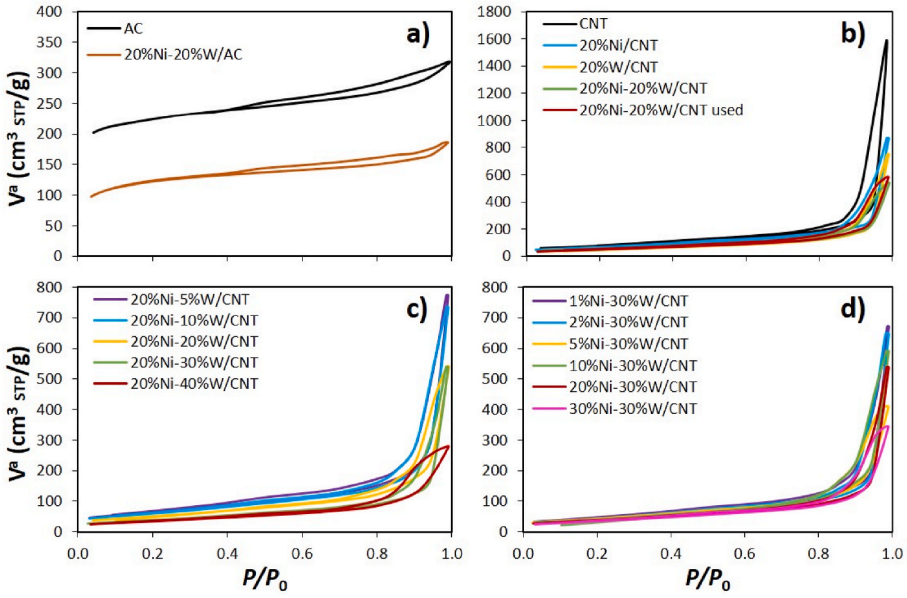

Fig. 3. N_2 adsorption-desorption isotherms of a) AC and 20%Ni–20%W/AC, b) mono- and bimetallic fresh and used catalysts supported on CNT, c) 20%Ni-y%W/CNT catalysts and d) x%Ni–30%W/CNT catalysts.

Table 3
Proximate analysis of the supports and catalysts.

Catalyst	Volatile matter (%)	Carbon fixed (%)	Ash (%)
CNT	32.0	57.1	10.9
20%Ni/CNT	24.7	39.4	35.9
20%W/CNT	13.0	53.1	33.9
1%Ni–30%W/CNT	21.0	37.0	42.0
2%Ni–30%W/CNT	19.0	38.4	42.6
5%Ni–30%W/CNT	18.0	36.8	45.2
10%Ni–30%W/CNT	17.0	26.9	56.1
20%Ni–30%W/CNT	15.0	18.5	66.5
30%Ni–30%W/CNT	18.3	10.5	71.2
20%Ni–5%W/CNT	13.0	45.4	41.6
20%Ni–10%W/CNT	9.5	50.5	40.0
20%Ni–20%W/CNT	23.0	22.5	54.5
20%Ni–40%W/CNT	19.0	8.2	72.8
20%Ni–20%W/CNT used	22.0	25.1	52.9
AC	7.0	77.1	15.9
20%Ni–20%W/AC	16.0	19.8	64.2

Table 4
Metal content of the prepared catalysts.

Catalyst	Ni ± 2 (wt. %)	W ± 4 (wt. %)
20%Ni/CNT	23	–
20%W/CNT	–	23
1%Ni–30%W/CNT	1	30
2%Ni–30%W/CNT	2	30
5%Ni–30%W/CNT	4	30
10%Ni–30%W/CNT	16	29
20%Ni–30%W/CNT	25	31
30%Ni–30%W/CNT	32	28
20%Ni–5%W/CNT	26	5
20%Ni–10%W/CNT	21	8
20%Ni–20%W/CNT	25	19
20%Ni–40%W/CNT	25	37
20%Ni–20%W/CNT used	23	19
20%Ni–20%W/AC	25	23

higher than the theoretical value. The loading of tungsten was estimated based on the total ashes of the metal catalysts and carbon support obtained by TG and the ICP results for Ni loading. Unlike Ni, the content of W estimated was, in general, slightly lower than the theoretical value. Furthermore, the metal composition of the 20%Ni–20%W/CNT catalysts before and after reaction (6 successive runs) was practically the same.

The synthesized catalysts were characterized by XRD (Fig. 4) to find factors that might be responsible for promoting interaction between both nickel and tungsten species. No amorphous diffraction peaks could be observed. The most evident diffraction peaks at about $2\theta = 43.7$, 51.8 and 75.6° are assigned to reduced nickel [44], while the characteristic tungstic crystallites appeared clearly at about 2θ = 25.9, 35.6, 36.7, 39.6, 40.9, 52.7, 58.1, 59.6, 62.2, 66.5, 69.5, 72.9 and 75.0°, attributed to tungsten species including W, WO_2 and W_3O. Although both WO_2 and W peaks were identified, WO_2 showed to dominate the catalyst composition since its characteristic peaks were much stronger than those of W. Additionally, some peaks corresponding to NiW alloys are present at about $2\theta = 30.8$ and 33.1°. These results are in agreement with those reported in the literature [15,16,19,24,34,42]. Furthermore, no notable change was observed between the fresh and used 20% Ni–20%W/CNT catalyst after 6 successive runs (Fig. 4a).

According to the XRD patterns of 20%Ni-(y)W/CNT catalysts with different W loadings, all catalysts exhibit the characteristic diffraction peaks of metallic nickel due to the formation of metal Ni crystallites, confirming the efficiency of the reduction step (Fig. 4b). However, with further increasing W loading up to 40%, a corresponding increase of the tungstic characteristic peaks mainly at $2\theta = 25.9$, 36.7, 52.7 and 66.5° was observed (Fig. 4b). This increase in the intensity of WO_2 and W_3O diffraction peaks with the increase of W loading is indicative of agglomeration of tungstic species on the catalyst. In addition, considering the higher Ni loadings, the metal may cover the active sites of W, which could weaken the catalytic ability to selective cleavage C–C bonds; to evaluate this possibility, catalysts with various Ni loadings were prepared maintaining a W content of 30%. For the 10%Ni–30%W/CNT and 20%Ni–30%W/CNT catalysts, the WO_2 reflections appeared at 25.9, 36.7, 52.7 and 59.6°, along with nickel peaks at 43.7, 51.8 and 75.6°, while 30%Ni–30%W/CNT also showed metal W characteristic peaks at 40.9 and 72.9°. With the increase of Ni loading from 10 to 30%, an increase in Ni peaks was noticeable followed by a decrease in WO_2 and W_3O reflections. When the Ni loading was 30%, there was a strong interaction between both metals resulting in more evidenced NiW alloy peaks at 30.8 and 33.1°.

SEM images were recorded in different magnifications to evaluate the influence of nickel and tungsten loadings on the morphology of the prepared catalysts, and are shown in Figs. 5 and 6, respectively. Moreover, EDS was also used to investigate the elemental composition of the catalysts, which confirmed the presence of Ni and W elements in all bimetallic catalysts. Comparing the catalysts prepared with different Ni contents, the metal particles in 1%Ni–30%W/CNT and 2%Ni–30%W/CNT are seemingly less homogeneously distributed compared to those of the other samples with higher Ni loadings, showing some larger particles that might result from tungsten particles agglomeration (Fig. 5a and b). With the increase of the amount of Ni to 5, 10 and 20% (Fig. 5c, d and e), the metal particles appear to be, in general, more uniformly distributed on the surface of carbon nanotubes. At the maximum loading considered (30%Ni–30%W/CNT), the excess of metallic particles on the support is evident, the carbon nanotubes being barely visible (Fig. 5f).

Evaluating the effect of the amount of W on the catalyst morphology, the distribution of Ni and W particles showed to be more concentrated in several areas at lower W loadings (i.e., 5 and 10%) (Fig. 6a and b). Again, with the increase of the tungsten content to 20 and 30%, it was possible to observe that both metal particles appear to be better dispersed over the CNT surface (Fig. 6c and d). Also, from the SEM image of 20%Ni–40%W/CNT, it was once again more noticeable the high coverage of carbon nanotubes with metal particles (Fig. 6e).

Finally, the monometallic catalysts, the catalyst recovered after utilization for 6 successive reaction tests and the Ni–W catalyst supported on AC were also analysed, and the respective microscopy images are presented in Fig. 7. The elementary composition from EDS revealed Ni or W phases in the respective monometallic catalysts. In the case of the Ni monometallic catalyst, it is clear that the nickel particles are uniformly dispersed on the CNTs (Fig. 7a), while relative large particles can be seen in the W monometallic catalyst due to particle agglomeration (Fig. 7b). On the other hand, the AC supported metallic particles are relatively larger than those of 20%Ni–20%W/CNT (Fig. 7d). To conclude, comparing the 20%Ni–20%W/CNT catalyst before (Fig. 6c) and after use (Fig. 7c), an obvious change can be noticed since the used sample presents some sort of a shield on the surface that might result from agglomeration of reaction products on the catalyst during reaction, as discussed later (see Section 3.2.2). In fact, other groups have already faced a decline in catalytic activity caused by reaction species accumulation on the catalyst surface, originating possible blockage of the active sites [19,37].

3.2. Cellulose conversion

Multivarious catalysts were evaluated on the conversion of cellulose directly into ethylene glycol. Besides the main product (EG), various side products were formed, many of them in minor amounts, such as sorbitol, propylene glycol, glycolaldehyde, glycerol, formic acid, levulinic acid and others. However, to simplify, the discussion of results will be mostly limited to the main product EG.

Firstly, a blank experiment (without catalyst) was carried out. Only traces of polyols were obtained after 5 h of reaction, with no EG detected, but the conversion of cellulose reached 56%, indicating that the H^+ produced in liquid hot water can hydrolyse cellulose to glucose.

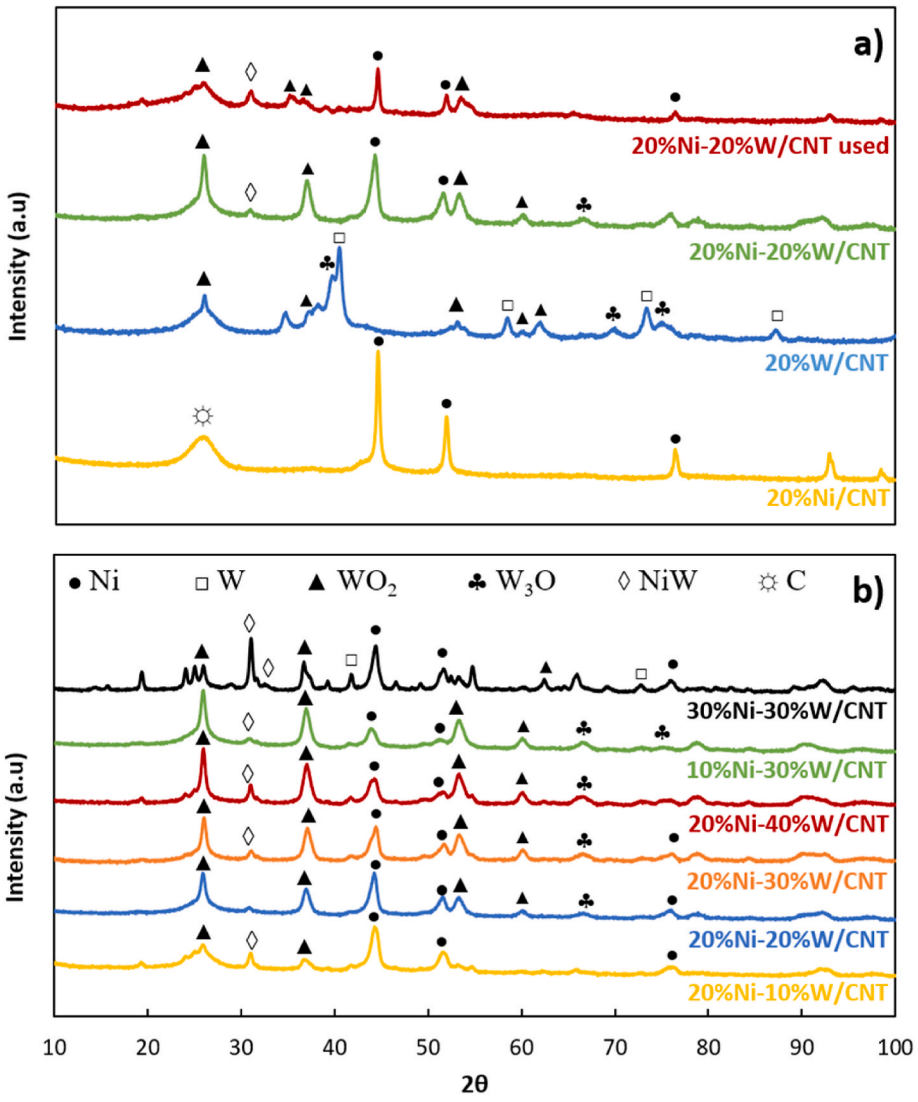

Fig. 4. XRD patterns of a) 20%Ni/CNT, 20%W/CNT, 20%Ni–20%W/CNT and 20%Ni–20%W/CNT used after 6 successive tests, and b) x%Ni-y%W/CNT catalysts. The legends in b) apply to the entire figure.

Also, when using only the support (CNT) as catalyst, despite the conversion of cellulose increased to 91%, EG was still not detected and the polyols yield remained low due to the lack of reactive active sites [36]. In both cases, cellulose was converted into unknown products such as humins, which was confirmed by the color change of the liquid mixture during reaction (Fig. 8). When a metal supported catalyst was used, regardless of the metal(s), a colourless liquid mixture was obtained throughout the entire reaction time under the same reaction conditions (Section 2.5), as depicted in Fig. 8.

Furthermore, the effect of the pre-treatment of the substrate was also analysed. Without ball-milling of cellulose prior to the reaction, the yield of EG attained over 20%Ni–20%W/CNT was only 27.7%, with a cellulose conversion of 56% after 5 h of reaction. The fact that microcrystalline cellulose was used without any pre-treatment led to a final conversion similar to that obtained without any catalyst and lower than that obtained using only CNT as catalyst, in the case of the conversion of ball-milled cellulose. Accordingly, all following experiments were conducted using a ball-milled substrate, in order to decrease its crystallinity and facilitate its conversion.

3.2.1. *Effect of catalytic properties*

Initially, W-catalyst-free experiments were performed, and it was observed that in the absence of W species, the dominant products were sugar alcohols, especially sorbitol. Indeed, using 20%Ni/CNT as catalyst, the conversion of cellulose and the yield of sorbitol attained after 5 h of reaction were 90 and 32.8%, respectively, ascribed to the high hydrogenation performance of Ni, while the yield of EG was only 5.4% (Fig. 9). In the opposite test, using a Ni-free catalyst (20%W/CNT), the conversion of cellulose was 94% and the yield of sorbitol greatly decreased to 1.8%, whereas the EG yield was raised to 18.0%, owing to the acid sites offered by W species (Fig. 9). Accordingly, the presence of W species is fundamental to shift the reaction route and favour RAC of glucose to glycolaldehyde (Fig. 1: route 2) in detriment of glucose hydrogenation to sugar alcohols or isomerization to fructose (Fig. 1: routes 1 and 3). Similarly, using Ni–W bimetallic catalysts, EG was the main product formed and the yield obtained was much higher. To determine whether this enhancement was either due to an intimate contact between W and Ni or to the presence of both metals, we mixed the 20%Ni/CNT and 20%W/CNT monometallic catalysts mechanically and then tested the mixture for cellulose conversion under the same reaction conditions. An EG yield of 43.0% was produced over the mixed catalysts (Fig. 9), in contrast to the EG yield of 50.3% over the 20%Ni–20%W/CNT bimetallic catalyst, suggesting that a synergistic effect between Ni and W is a key to attain high EG yields.

Afterwards, the effect of the support was also investigated. The poor EG yield of 8.2% obtained using 20%Ni–20%W/AC compared to that of

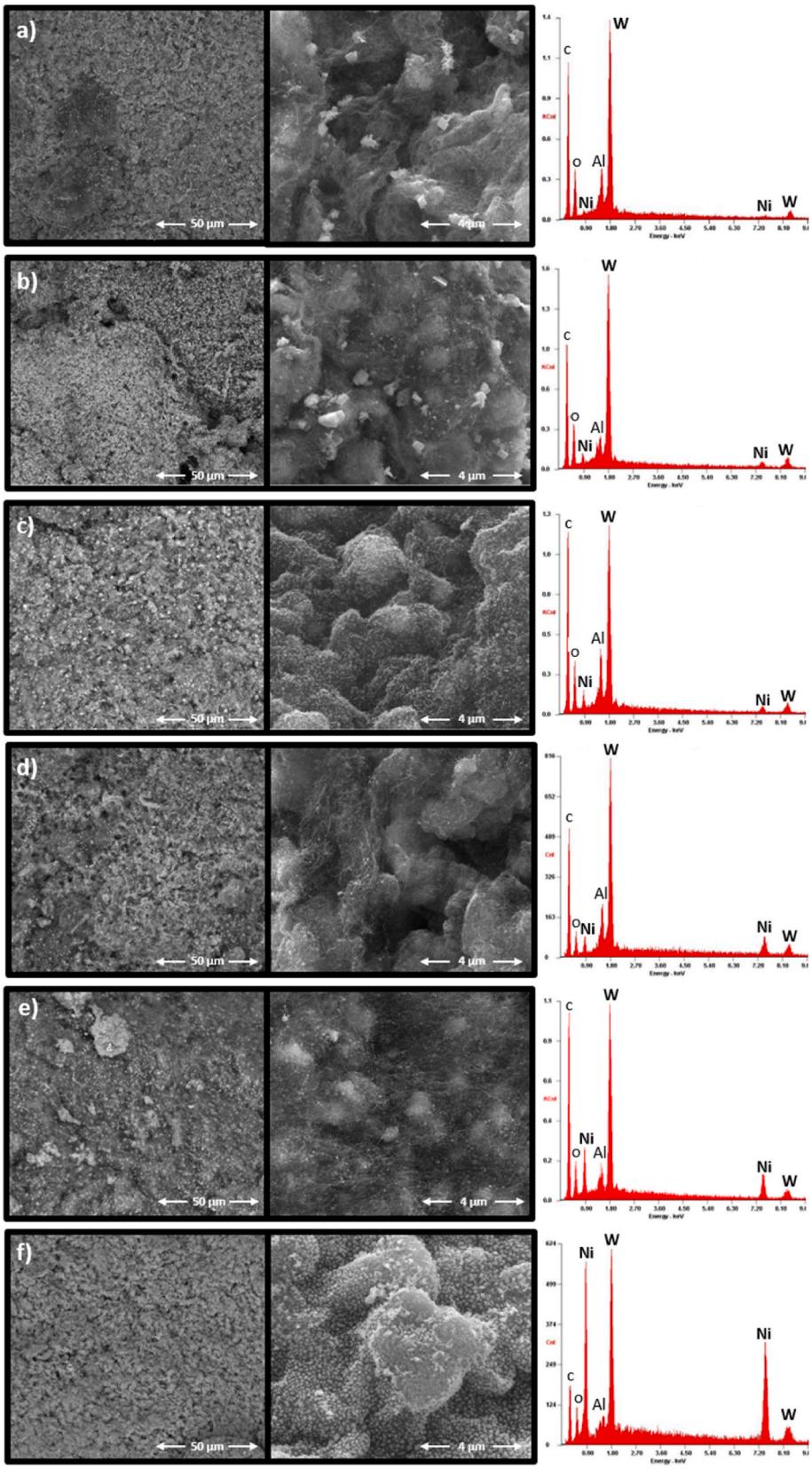

Fig. 5. SEM images (× 2000 and × 25000 magnifications) and EDS analysis of a) 1%Ni–30%W/CNT, b) 2%Ni–30%W/CNT, c) 5%Ni–30%W/CNT, d) 10%Ni–30%W/CNT, e) 20%Ni–30%W/CNT and f) 30%Ni–30%W/CNT.

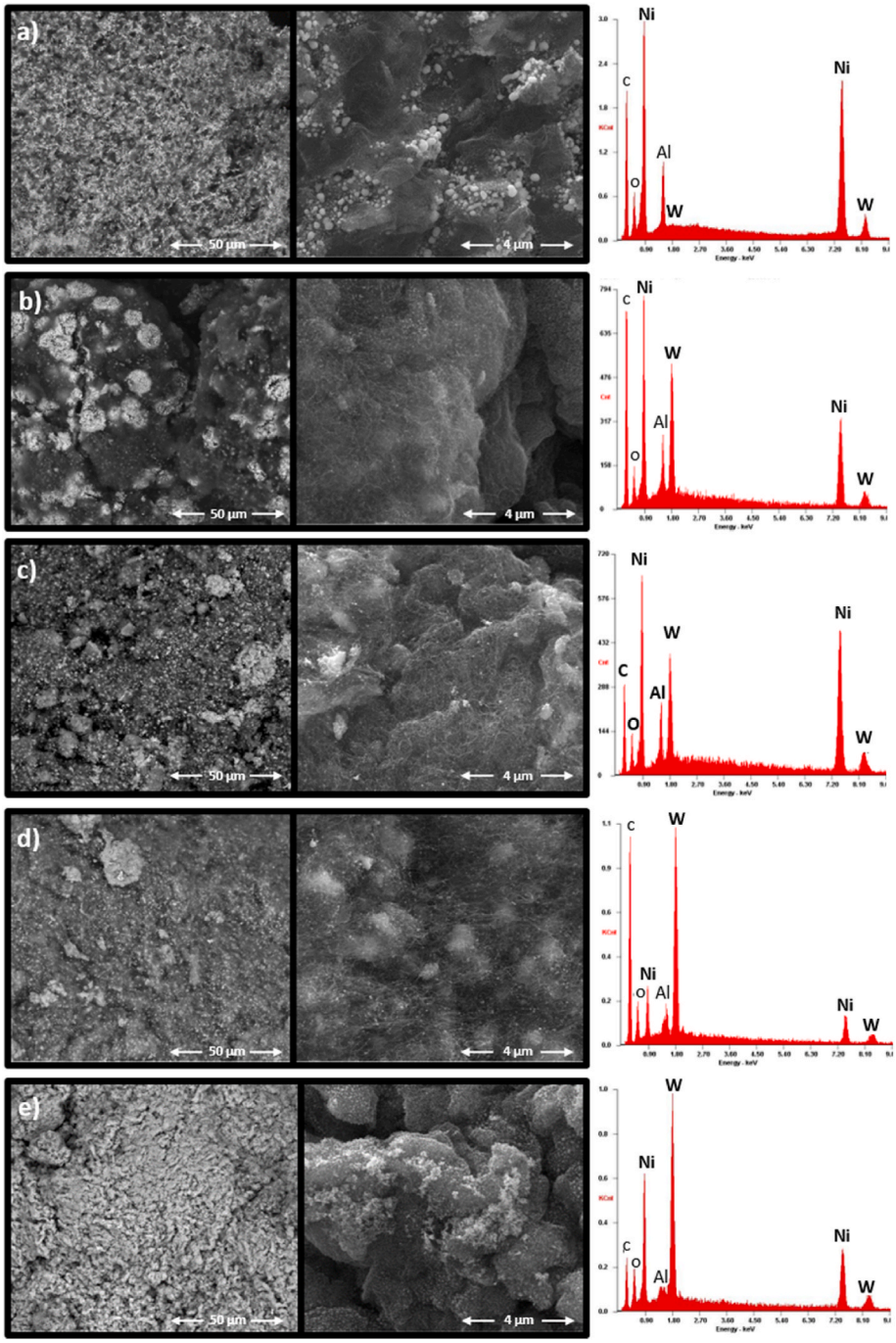

Fig. 6. SEM images (× 2000 and × 25000 magnifications) and EDS analysis of a) 20%Ni–5%W/CNT, b) 20%Ni–10%W/CNT, c) 20%Ni–20%W/CNT, d) 20%Ni–30% W/CNT and e) 20%Ni–40%W/CNT.

50.3% reached over 20%Ni–20%W/CNT might be related to the different porosity structures (observed in Section 3.1), since the metal loadings of the two catalysts are very similar (Table 4). In this case, the microporous structure of 20%Ni–20%W/AC might limit the transport of oligosaccharides into the channels, hindering further hydrogenation reactions, in contrast to the mesoporous structure of 20%Ni–20%W/CNT that might be beneficial to this transport. Li et al. have also concluded that a suitable mesoporous structure of Ni–W catalysts supported on MIL-125(Ti) was beneficial for enhancing the catalytic activity when compared to Ni–W/AC [1]. Based on these results, it can be concluded that the support has a noticeable effect on the catalytic activity and selectivity related to different surface areas and pore distributions. Accordingly, the subsequent experiments were conducted using carbon nanotubes supported Ni–W bimetallic catalysts.

Since in this reaction the two crucial steps involved in EG production from cellulose are the C–C bond cleavage on active tungsten sites and the hydrogenation of intermediates on nickel sites, we investigated next the influence of Ni and W loadings on the conversion of cellulose and yield of EG, and the results are presented in Fig. 10. Full data concerning these tests can also be accessed in the Supplementary Information (Figs. S1–S7). Although high Ni loading can boost hydrogenation, it is important to notice that this metal may cover part of the active sites of tungsten species; therefore, to achieve a high EG selectivity, the optimization of the ratio between Ni and W is of utmost importance. We started to study the effect of Ni loading maintaining a 30 wt% tungsten content and varying the Ni amount from 1 to 30 wt% (Fig. 10a). The

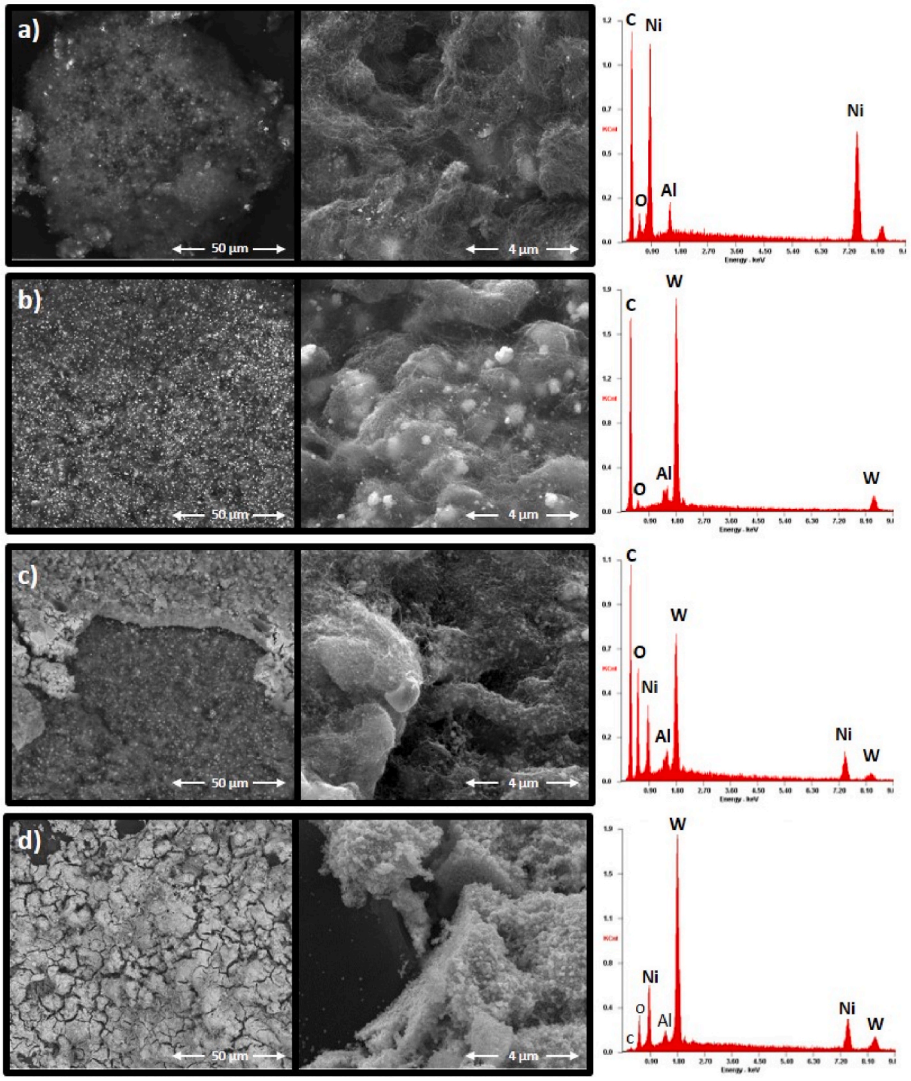

Fig. 7. SEM images (× 2000 and × 25000 magnifications) and EDS analysis of a) 20%Ni/CNT, b) 20%W/CNT, c) 20%Ni–20%W/CNT after 6 runs and d) 20% Ni–20%W/AC.

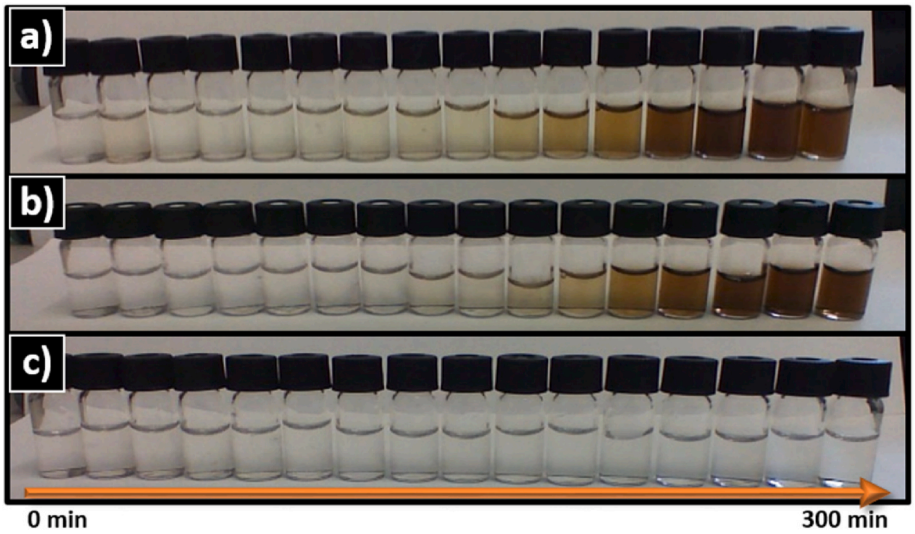

Fig. 8. Evolution of the reaction mixture color with the reaction time over a) no catalyst, b) CNT and c) 20%Ni–20%W/CNT.

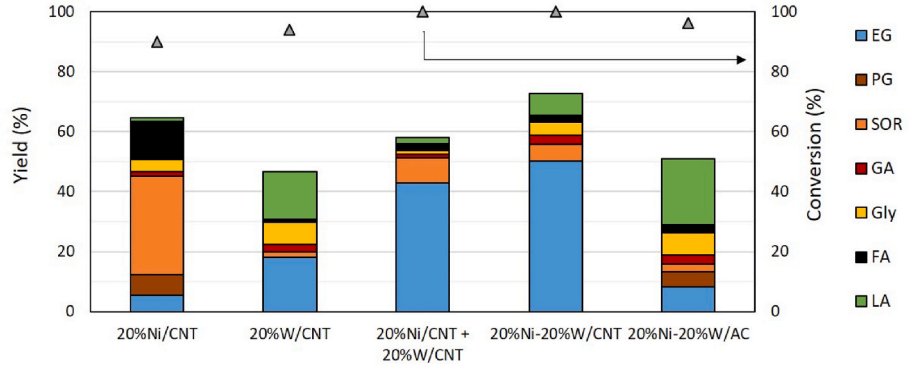

Fig. 9. Effect of metal phase and catalytic support. Reaction conditions: ball-milled cellulose (0.75 g), catalyst (0.3 g), water (0.3 L), 205 °C, 50 bar of H_2, 300 rpm, 5 h. EG, PG, SOR, GA, Gly, FA and LA are abbreviations for ethylene glycol, propylene glycol, sorbitol, glycolaldehyde, glycerol, formic acid and levulinic acid, respectively.

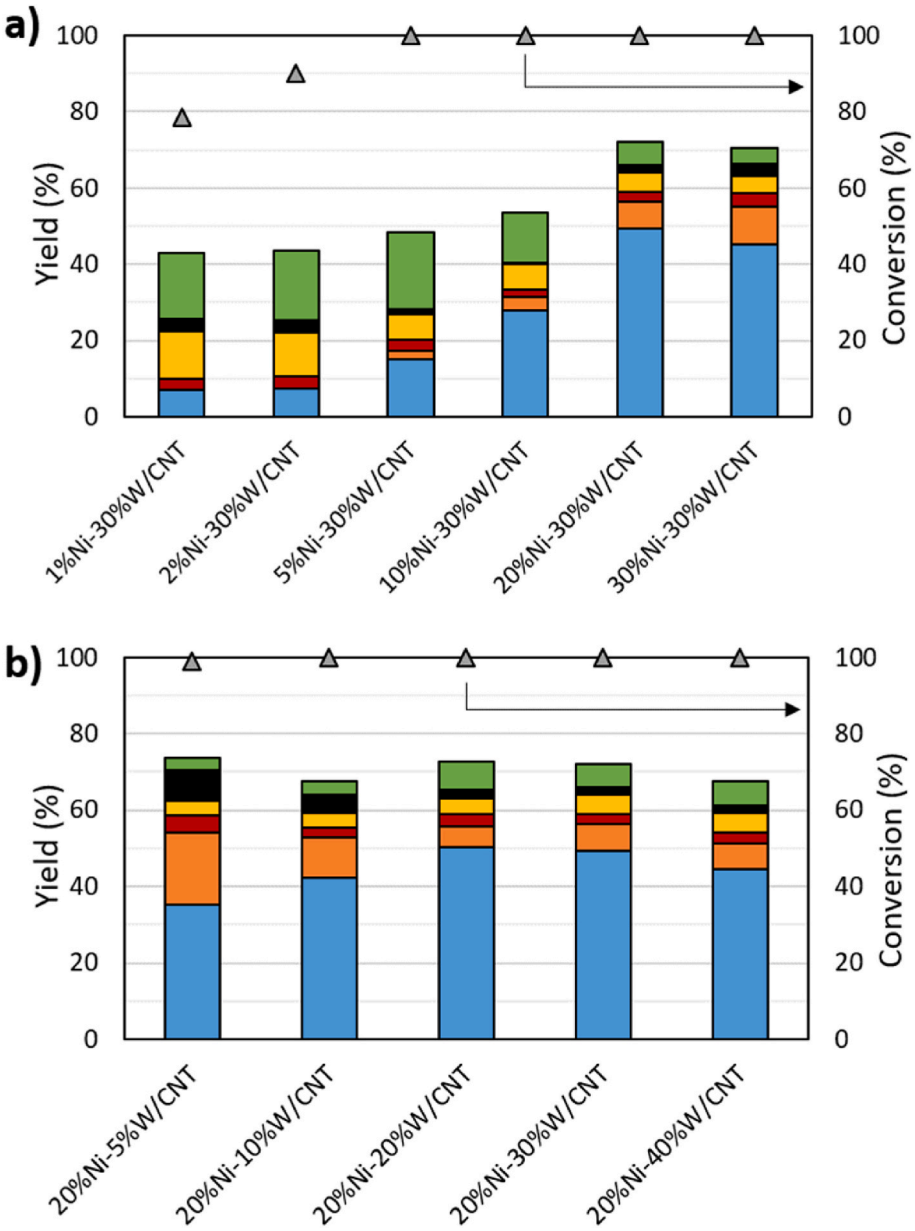

Fig. 10. Effect of a) Ni and b) W loadings. Reaction conditions: ball-milled cellulose (0.75 g), catalyst (0.3 g), water (0.3 L), 205 °C, 50 bar of H_2, 300 rpm, 5 h. EG, SOR, GA, Gly, FA and LA are abbreviations for ethylene glycol, sorbitol, glycolaldehyde, glycerol, formic acid and levulinic acid, respectively.

conversion of cellulose increased from 79 to 100% with the Ni content increase from 1 to 5 wt% and kept at 100% with further increase of Ni loading. On the other hand, the yield of EG improved with the rise of Ni loading, reaching a maximum (49.3%) at 20% loading. This increase is related to the fact that Ni is the metal responsible for hydrogenation, providing more hydrogenation sites at higher loadings, which also increased the yield of hydrogenation products like sorbitol. However, further increase of Ni loading to 30 wt% originated a slight decline in the yield of EG to 45.2%, which might result from two reasons: i) higher Ni loading generates more hydrogenation active sites that compete with W, leading to the non-selective cleavage of C–C bond, and ii) excessive nickel can block part of the W sites, which could be verified by the catalyst characterization results (Section 3.1). The inferior performance of 30%Ni–30%W/CNT compared to that of 20%Ni–30%W/CNT is also explained by XRD results since the catalyst with excess Ni presented more evidenced NiW and W peaks in detriment of Ni, W_3O and WO_2 peaks (Fig. 4b), suggesting that the excess Ni led to the formation of NiW, decreasing the number of active Ni sites. All the above results explain that the excess of Ni can have a negative impact on the production of EG. In conclusion, the maximum EG yield was attained over 20%Ni–30%W/CNT.

According to the previous results, the influence of W loading was then examined by varying its content from 5 to 40 wt% and fixing the Ni loading at 20 wt %. For the W-free catalyst, the primary product was sorbitol with a yield of 32.8%, and only 5.4% yield of EG. In contrast, by adding even a minor amount of W to the catalyst (5%), the yield of EG was greatly increased, up to 35.1%, while the sorbitol yield decreased to 18.9%. With the rise of W loading, the conversion of cellulose was 100% in all cases, but the yield of EG showed a maximum of 50.3%, which was reached at 20% W loading (Fig. 10b). The SEM analysis (Fig. 6) revealed that a high loading of W induces agglomeration, causing lower catalytic performance. Using an insufficient amount of tungsten (5 wt %), a large formation of hydrogenation products like sorbitol was noticed, confirming that W species play a fundamental role in the bond cleavage of glucose via retro-aldol condensation. In fact, 20%Ni–20%W/CNT outperformed the other tested catalysts since it enabled the best equilibrium between retro-aldol condensation and hydrogenation reactions due to the optimal conjugation of nickel and tungsten active sites, and also since it corresponds to the catalyst with none or minimum NiW diffraction peaks in comparison with all remaining bimetallic catalysts.

These results demonstrate that excessive Ni or W loading has a negative impact on the catalytic performance for the direct conversion of cellulose to EG. The intimate interaction of the two metals (i.e., the formation of alloys) is detrimental to this reaction. Both active sites are important for the process since W can promote the RAC reaction while Ni promotes the subsequent hydrogenation. In fact, it can be concluded that the most efficient catalyst for maximized production of EG is 20% Ni–20%W/CNT, since it provided the best combination of W and Ni active sites that was enough to avoid particles agglomeration and to favour the conversion of glucose to glycolaldehyde and its subsequent hydrogenation to EG (Fig. 1: route 2) without further hydrogenation to side products. As a result, this catalyst was selected for the subsequent studies.

Cellulose conversion can follow different pathways (see Fig. 1). Therefore, the main key to enhance the yield of EG is to balance the reaction rates of cellulose hydrolysis, retro-aldol condensation, and hydrogenation, by optimizing the contents of Ni and W. As evidenced in Fig. 10, there is a significant difference in the product distribution when using different Ni and W contents. The yield of sorbitol increased with the rise of Ni loading, since Ni enhances the hydrogenation reaction, promoting route 1 in Fig. 1. On the other hand, the yield of sorbitol was higher for insufficient W loading (5 wt %), suggesting that route 1 was favoured, but when W was present in higher amounts, route 2 was favoured over route 1 (see Fig. 1), leading to the preferential formation of EG. The difference observed between the results obtained with low and high W contents clearly confirms that tungsten promoted route 2 in which RAC of glucose to GA was the key step. Although the high Ni loading is beneficial to boost hydrogenation, it might also compete with W and lead to the non-cleavage of C–C bond and/or cover part of the tungsten species required for RAC in order to favour route 2. So, taking into account the evolution of the reaction during the 5 h for the different Ni/W ratios (Figs. S1–S7), it was evident the positive effect that the increase of the Ni content had on the yields of EG and sorbitol due to its hydrogenation properties, in contrast to the negative effect on the yields of glycerol and levulinic acid, while the production of formic acid was not significantly affected by the Ni content. On the other hand, the increase of the W loading was unfavourable to the formation of sorbitol and formic acid, and had practically no effect on the production of EG or glycerol. In fact, analysing the first 30 min of reaction, we can verify that the increase in the amount of W active sites results in an increase of the glycolaldehyde yield, due to the promotion of the C–C cleavage. Based on these results, the reaction route for cellulose conversion to EG can be proposed: i) cellulose hydrolysis into glucose favoured by H+ species from hot liquid water, ii) glucose C–C bond cleavage into glycolaldehyde promoted by W sites, and iii) glycolaldehyde hydrogenation to EG over Ni metal sites (route 2 in Fig. 1). In summary, W acted on RAC reaction while Ni worked on hydrogenation, thus the favourability of route 2 and maximization of the synergistic effect of C–C bond cleavage and hydrogenation being achieved by the adjustment of the Ni/W ratio.

A proper comparison between the results herein obtained with those previously reported is extremely difficult due to the different reaction parameters involved. In general, the vast majority of results reported in the literature were obtained at temperatures higher than 240 °C and hydrogen pressures higher than 60 bar. In this work, we accomplished the conversion of cellulose to EG with a 50.3% yield after 5 h at only 205 °C and 50 bar of H_2 (*P* measured at 205 °C). The most similar catalytic conditions are probably those of Xiao et al. who obtained 100% cellulose conversion with an EG yield of 55% over 15%Ni–20%W/CNT at 240 °C and 50 bar of H_2 (*P* measured at room temperature) [34]. Likewise, Liu et al. attained a 57% EG yield with 100% cellulose conversion over 30%NiWB(3:1)/CNT at 250 °C and 60 bar of H_2 (*P* measured at room temperature) [19]. These yields are similar to that obtained in the present work, but the conditions used by Xiao's and Liu's groups were considerably more drastic. Yet, comparing within the same reaction conditions, here we were able to surpass previous results obtained using more expensive Ru–W/CNT catalysts [35,36]. Namely, in our previous works, we had concluded that Ru–W supported on commercial carbon nanotubes had excellent performance for the conversion of cellulose and cellulosic materials to glycols, especially ethylene glycol with a yield of EG around 40% [13,36]. In the present work, we switched from Ru to non-noble Ni, which allowed to overcome that previous result under the same conditions.

3.2.2. Recyclability

A fundamental key to the practical application of catalysts in metal-catalysed liquid-phase reactions is its stability and reusability due to two main reasons: 1) possible metal leaching to solution, which is attributed to the H^+ formed in hot water, and 2) possible blockage of pores and poisoning of the catalyst due to the production of complex intermediates in side reactions. Therefore, six recycling tests were conducted using a sample of the best catalyst (20%Ni–20%W/CNT). For the recycling tests, the catalyst was recovered after reaction by filtration, washed with deionized water and dried overnight at 100 °C. Due to some mass losses during the recovering process, a small amount of fresh catalyst (<5 wt %) was added before each test.

The conversion of cellulose and product yields after 5 h of reaction are displayed in Fig. 11. Neither the conversion nor the EG yield decreased drastically after each cycle, indicating that 20%Ni–20%W/CNT maintained good activity without important deactivation. Since the catalyst deactivation is generally due to metal leaching, atomic absorption spectroscopy of the liquid recovered after reaction was conducted to determine the amount of Ni and/or W leaching to solution.

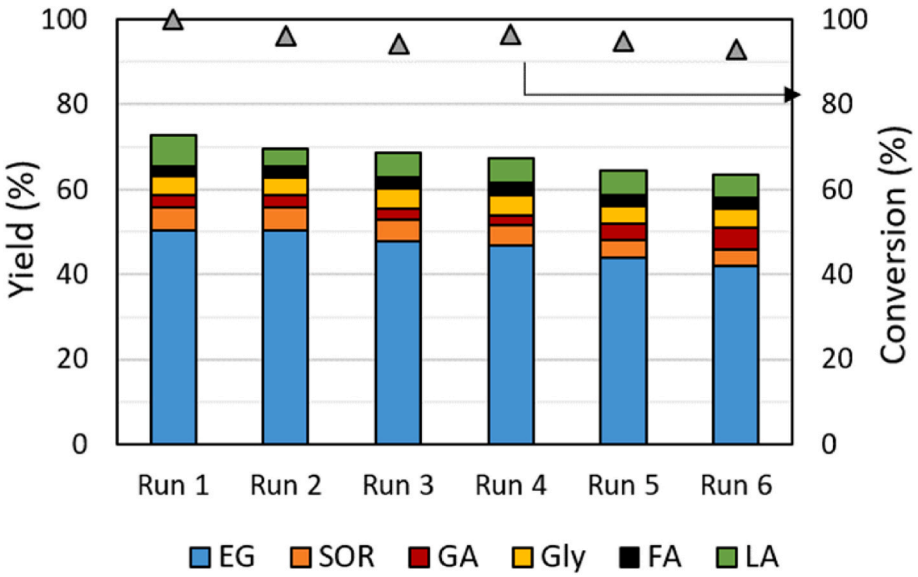

Fig. 11. Recycling tests of 20%Ni–20%W/CNT. Reaction conditions: ball-milled cellulose (0.75 g), 20%Ni–20%W/CNT (0.3 g), water (0.3 L), 205 °C, 50 bar of H_2, 300 rpm, 5 h. EG, SOR, GA, Gly, FA and LA are abbreviations for ethylene glycol, sorbitol, glycolaldehyde, glycerol, formic acid and levulinic acid, respectively.

The results indicated that the metals leaching was negligible (under the detection limits), which can justify the reasonable catalytic activity during the six successive tests.

To further study the stability of 20%Ni–20%W/CNT, the composition and structure of the catalyst recovered after the six cycles was characterized by N_2 adsorption isotherms, TG, ICP, XRD and SEM/EDS. No significant changes were observed in all characterization results, except for microscopy (Section 3.1). The textural properties and XRD patterns before and after reaction did not change significantly (Fig. 3, Table 2 and Fig. 4), while ICP and thermogravimetric results before and after reaction were practically the same (Tables 3 and 4), suggesting that the catalyst did not suffer important structural changes. On the other hand, SEM images evidenced some agglomeration of products on the catalyst after reaction (Fig. 7), which might justify the decrease obtained for the EG yield from 50.3 to 42.0% after the six runs, due to possible blockage of the catalytic sites. This phenomenon was also observed by Yang's and Liu's groups, who confirmed that the activity decline was caused by accumulation of reaction species on the catalyst surface [19, 37].

3.3. Valorisation of lignocellulosic wastes

Since biomass conversion to value-added chemicals is one of the most challenging and important advances of green chemistry needed in industry, after determining the best performing catalyst for EG production directly from cellulose, it was evaluated for the direct conversion of lignocellulosic materials that can be considered as wastes. Three substrates were selected in order to test three different kinds of residues: forestry (eucalyptus wood), agricultural (corncob) and urban (cotton wool). As expected, the conversion of cellulose and yield of EG attained are lower than those obtained directly from cellulose, due to the recalcitrant lignocellulosic structure (Fig. 12). Besides that, part of lignin can undergo degradation and repolymerization, and might cover or poison the catalyst hydrogenation sites, originating lower EG yields [24]. Consequently, the highest conversion and EG yield (93% and 43.1%, respectively) were obtained from cotton wool, since it is mainly composed of cellulose, unlike corncob and eucalyptus wood that contain 27.6 and 25.7% of lignin, respectively [38]. Yet, conversions of 76 and 67% and EG yields of 36.3 and 27.8% could be produced directly from

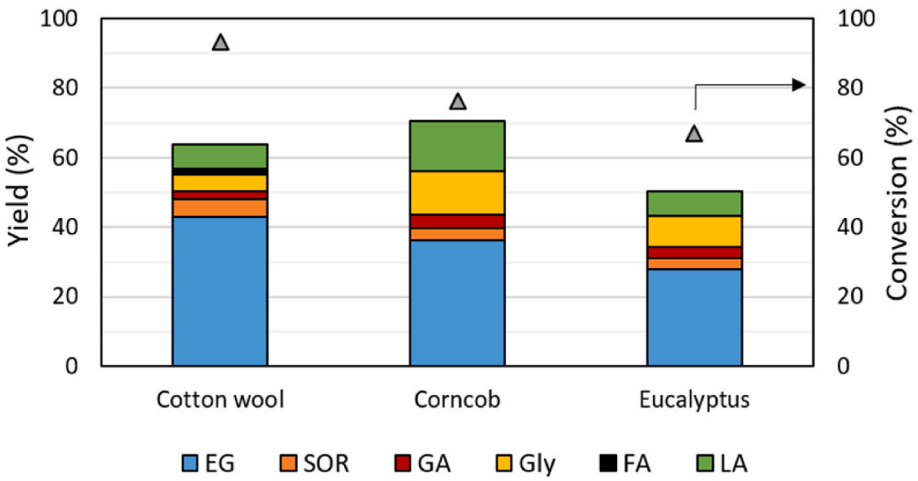

Fig. 12. Catalytic results of waste lignocellulosic biomass materials conversion [Yields obtained from corncob and eucalyptus were calculated based on the respective holocellulose fraction]. Reaction conditions: ball-milled substrate (0.75 g), 20%Ni–20%W/CNT (0.3 g), water (0.3 L), 205 °C, 50 bar of H_2, 300 rpm, 5 h. EG, SOR, GA, Gly, FA and LA are abbreviations for ethylene glycol, sorbitol, glycolaldehyde, glycerol, formic acid and levulinic acid, respectively.

corncob and eucalyptus wood, respectively, without any pre-treatment besides ball-milling. These lignocellulosic residues conversion results are in accordance with our assumption that EG can only be produced from cellulose and hemicellulose (see Section 2.6) since the amount of unconverted eucalyptus wood and corncob is similar to their lignin content. Again, it is extremely difficult to compare these results with those previously reported due to the different reaction parameters involved, especially since the substantial majority of results reported in the literature were obtained under much more drastic conditions (>240 °C and >60 bar of H_2). In addition, only a few works have reported the conversion of biomass into EG over carbon-supported catalysts. Pang's group attained an EG yield of 18% from cornstalk over 2% Ni–30%W_2C/AC at 245 °C after 2 h [45], and later an EG yield of 51% from pre-treated corncob cellulose at 245 °C and 65 bar of H_2 (P measured at room temperature) after 3 h over tungstic acid and Raney Ni [46]. Furthermore, Li et al. accomplished an EG yield of 51% from birch wood over 4%Ni–30%W_2C/AC at 245 °C after 2 h [47]. Our team has also tested the conversion of various biomass residues over a combination of Ru and W catalysts supported on CNT [38]. The highest EG yields of more than 40% were achieved from eucalyptus wood and cotton wool, while corncob and tissue paper produced EG yields of 24 and 34%, respectively [38]. In the present work, we managed to surpass the results obtained from cotton wool and corncob using cheaper Ni–W catalysts, though the yield of EG obtained from eucalyptus wood was lower.

4. Conclusions

Cellulose and lignocellulosic residues such as cotton wool, corncob and eucalyptus wood were converted using cheap and non-toxic water as reaction media. Ball-milling was used as a sustainable pre-treatment of substrates to facilitate the process, in replacement of mineral acids. Stable Ni–W-based catalysts supported on carbon nanotubes were synthesized for the direct production of EG; they were fully characterized before and after reaction by different techniques including TG, SEM, EDS, XRD, ICP and N_2 adsorption. The Ni–W/CNT bifunctional catalysts were used to catalyse not only the hydrogenation but also the hydrolysis and RAC reaction, allowing to maximize the yield of the main product (EG) through a balance of the catalytic efficiency towards the reaction steps mentioned above.

To conclude, an appropriate ratio between Ni and W active sites ensured a well synergetic effect of C–C cleavage and hydrogenation capabilities, thus resulting in an EG yield over 50% directly from ball-milled cellulose over 20%Ni–20%W/CNT at 205 °C and 50 bar of H_2 after 5 h. Furthermore, compared with previously reported catalysts, this catalyst showed reasonable stability and recyclability. Forestry (eucalyptus wood), agricultural (corncob) and urban (cotton wool) residues were also directly converted into EG with yields of 27.8, 36.3 and 46.1%, respectively. Considering the practical application of the sustainable EG production from cellulose and biomass, 20%Ni–20%W/CNT is here presented as a potential cost-effective catalyst solution for the future: not only noble metals (e.g., Ru) were replaced by cheap earth-abundant metals (i.e., Ni), but also the catalyst possesses good stability under hydrothermal conditions.

CRediT authorship contribution statement

Lucília Sousa Ribeiro: Writing – original draft, Conceptualization. **Ana Luzia Ferreira Pires:** Investigation. **José Joaquim de Melo Órfão:** Writing – review & editing, Conceptualization. **Manuel Fernando Ribeiro Pereira:** Writing – review & editing, Conceptualization, Funding acquisition, Supervision.

Declaration of competing interest

The authors declare that they have no known competing financial interests or personal relationships that could have appeared to influence the work reported in this paper.

Data availability

Data will be made available on request.

Acknowledgements

This work was financially supported by LA/P/0045/2020 (ALiCE), UIDB/50020/2020 and UIDP/50020/2020 (LSRE-LCM), funded by national funds through FCT/MCTES (PIDDAC), and by project "Verãocom Ciência 2021", supported by Fundação para a Ciência e a Tecnologia (FCT).

Appendix A. Supplementary data

Supplementary data to this article can be found online at https://doi.org/10.1016/j.renene.2022.10.026.

References

[1] N. Li, X. Liu, J. Zhou, Q. Ma, M. Liu, W. Chen, Enhanced Ni/W/Ti catalyst stability from Ti–O–W linkage for effective conversion of cellulose into ethylene glycol, ACS Sustain. Chem. Eng. 8 (2020) 9650–9659.
[2] Y. Liang, Z. Li, Q. Liu, L. Ma, Selective xylose hydrogenolysis to 1,2-diols using Co@NC catalysts, J. Fuel Chem. Technol. 49 (2021) 1898–1910.
[3] G. Zhao, M. Zheng, A. Wang, T. Zhang, Catalytic conversion of cellulose to ethylene glycol over tungsten phosphide catalysts, Chin. J. Catal. 31 (2010) 928–932.
[4] Z. Xiao, Q. Ge, C. Xing, S. Fang, J. Ji, J. Mao, One-pot catalytic agroforestry waste cellulose to polyols over self-reducing bifunctional catalysts, J. Fuel Chem. Technol. 43 (2015) 1446–1453.
[5] J. Ahlkvist, S. Ajaikumar, W. Larsson, J. Mikkola, One-pot catalytic conversion of Nordic pulp media into green platform chemicals, Appl Catal A-Gen 454 (2013) 21–29.
[6] L.S. Ribeiro, J.J. Delgado, J.J.M. Órfão, M.F.R. Pereira, Influence of the surface chemistry of multiwalled carbon nanotubes on the selective conversion of cellulose into sorbitol, ChemCatChem 9 (2017) 888–896.
[7] A. Kumar Anu, A. Rapoport, G. Kunze, S. Kumar, D. Singh, B. Singh, Multifarious pretreatment strategies for the lignocellulosic substrates for the generation of renewable and sustainable biofuels: a review, Renew. Energy 160 (2020) 1228–1252.
[8] M. Gu, Z. Shen, L. Yang, W. Dong, L. Kong, W. Zhang, B. Peng, Y. Zhang, Reaction route selection for cellulose hydrogenolysis into C2/C3 glycols by ZnO-modified Ni-W/β-zeolite catalysts, Sci. Rep. 9 (2019), 11938.
[9] N. Ji, T. Zhang, M. Zheng, A. Wang, H. Wang, X. Wang, Y. Shu, A.L. Stottlemyer, J. G. Chen, Catalytic conversion of cellulose into ethylene glycol over supported carbide catalysts, Catal. Today 147 (2009) 77–85.
[10] Y. Cao, J. Wang, M. Kang, Y. Zhu, Catalytic conversion of glucose and cellobiose into ethylene glycol over various tunsgten-based catalysts, J. Fuel Chem. Technol. 44 (2016) 845–852.
[11] H. Kobayashi, Y. Yamakoshi, Y. Hosaka, M. Yabushita, A. Fukuoka, Production of sugar alcohols from real biomass by supported platinum catalyst, Catal. Today 226 (2014) 204–209.
[12] P.A. Lazaridis, S.A. Karakoulia, C. Teodorescu, N. Apostol, D. Macovei, A. Panteli, A. Delimitis, S.M. Coman, V.I. Parvulescu, K.S. Triantafyllidis, High hexitols selectivity in cellulose hydrolytic hydrogenation over platinum (Pt) vs. ruthenium (Ru) catalysts supported on micro/mesoporous carbon, Appl. Catal. B Environ. 214 (2017) 1–14.
[13] L.S. Ribeiro, J.J.M. Órfão, M.F.R. Pereira, Insights into the effect of the catalytic functions on selective production of ethylene glycol from lignocellulosic biomass over carbon supported ruthenium and tungsten catalysts, Bioresour. Technol. 263 (2018) 402–409.
[14] M.Y. Zheng, A.Q. Wang, N. Ji, J.F. Pang, X.D. Wang, T. Zhang, Transition metal-tungsten bimetallic catalysts for the conversion of cellulose into ethylene glycol, ChemSusChem 3 (2010) 63–66.
[15] Z. Xiao, Y. Fan, Y. Cheng, Q. Zhang, Q. Ge, R. Sha, J. Ji, J. Mao, Metal particles supported on SiO2-OH nanosphere: new insight into interactions with metals for cellulose conversion to ethylene glycol, Fuel 215 (2018) 406–416.
[16] N. Ji, T. Zhang, M. Zheng, A. Wang, H. Wang, X. Wang, J.G. Chen, Direct catalytic conversion of cellulose into ethylene glycol using nickel-promoted tungsten carbide catalysts, Angew. Chem., Int. Ed. 47 (2008) 8510–8513.
[17] L.S. Ribeiro, J.J.M. Órfão, M.F.R. Pereira, An overview of the hydrolytic hydrogenation of lignocellulosic biomass using carbon-supported metal catalysts, Mater Today Sust 11–12 (2021), 100058.
[18] T.D.J. Molder, S.R.A. Kersten, J.P. Lange, M.P. Ruiz, Ethylene glycol from lignocellulosic biomass: impact of lignin on catalytic hydrogenolysis, Ind. Eng. Chem. Res. 60 (2021) 7043–7049.

[19] H. Liu, L. Qin, X. Wang, C. Du, D. Sun, X. Meng, Hydrolytic hydro-conversion of cellulose to ethylene glycol over bimetallic CNTs-supported NiWB amorphous alloy catalyst, Catal. Commun. 77 (2016) 47–51.
[20] R. Sun, T. Wang, M. Zheng, W. Deng, J. Pang, A. Wang, X. Wang, T. Zhang, Versatile nickel–lanthanum(III) catalyst for direct conversion of cellulose to glycols, ACS Catal. 5 (2015) 874–883.
[21] Z. Xiao, J. Mao, J. Ji, R. Sha, Y. Fan, C. Xing, Preparation of nano-scale nickel-tungsten catalysts by pH value control and application in hydrogenolysis of cellulose to polyols, J. Fuel Chem. Technol. 45 (2017) 641–650.
[22] M.S. Hamdy, M.A. Eissa, S.M.A.S. Keshk, New catalyst with multiple active sites for selective hydrogenolysis of cellulose to ethylene glycol, Green Chem. 19 (2017) 5144–5151.
[23] Y. Liu, Y. Liu, Y. Zhang, The synergistic effects of Ru and WOx for aqueous-phase hydrogenation of glucose to lower diols, Appl. Catal. B Environ. 242 (2019) 100–108.
[24] G. Pan, Y. Ma, X. Ma, Y. Sun, J. Lv, J. Zhang, Catalytic hydrogenation of corn stalk into polyol over Ni–W/MCM-41 catalyst, Chem. Eng. J. 299 (2016) 386–392.
[25] J. Pang, M. Zheng, X. Li, J. Sebastian, Y. Jiang, Y. Zhao, A. Wang, T. Zhang, Unlock the compact structure of lignocellulosic biomass by mild ball milling for ethylene glycol production, ACS Sustain. Chem. Eng. 7 (2019) 679–687.
[26] L.S. Ribeiro, N. Rey-Raap, J.L. Figueiredo, J.J.M. Órfão, M.F.R. Pereira, Glucose-based carbon materials as supports for the efficient catalytic transformation of cellulose directly to ethylene glycol, Cellulose 26 (2019) 7337–7353.
[27] Z. Tan, L. Shi, Y. Zan, G. Miao, S. Li, L. Kong, S. Li, Y. Sun, Crucial role of support in glucose selective conversion into 1,2-propanediol and ethylene glycol over Ni-based catalysts: a combined experimental and computational study, Appl. Catal. Gen. 560 (2018) 28–36.
[28] A. Wang, T. Zhang, One-pot conversion of cellulose to ethylene glycol with multifunctional tungsten-based catalysts, Acc. Chem. Res. 46 (2013) 1377–1386.
[29] K. Zhang, G. Yang, G. Lyu, Z. Jia, L.A. Lucia, J. Chen, One-pot solvothermal synthesis of graphene nanocomposites for catalytic conversion of cellulose to ethylene glycol, ACS Sustain. Chem. Eng. 7 (2019) 11110–11117.
[30] R. Sun, M. Zheng, J. Pang, X. Liu, J. Wang, X. Pan, A. Wang, X. Wang, T. Zhang, Selectivity-switchable conversion of cellulose to glycols over Ni–Sn catalysts, ACS Catal. 6 (2016) 191–201.
[31] Y. Zhang, A. Wang, T. Zhang, A new 3D mesoporous carbon replicated from commercial silica as a catalyst support for direct conversion of cellulose into ethylene glycol, Chem. Commun. 46 (2010) 862–864.
[32] N. Ji, M. Zheng, A. Wang, T. Zhang, J.G. Chen, Nickel-promoted tungsten carbide catalysts for cellulose conversion: effect of preparation methods, ChemSusChem 5 (2012) 939–944.
[33] D. Chu, C. Zhao, Reduced oxygen-deficient CuWO4 with Ni catalyzed selective hydrogenolysis of cellulose to ethylene glycol, Catal. Today 351 (2020) 125–132.
[34] Z. Xiao, Q. Zhang, T. Chen, X. Wang, Y. Fan, Q. Ge, R. Zhai, R. Sun, J. Ji, J. Mao, Heterobimetallic catalysis for lignocellulose to ethylene glycol on nickel-tungsten catalysts: influenced by hydroxy groups, Fuel 230 (2018) 332–343.
[35] Y. Liu, H. Liu, Kinetic insight into the effect of the catalytic functions on selective conversion of cellulose to polyols on carbon-supported WO3 and Ru catalysts, Catal. Today 269 (2016) 74–81.
[36] L.S. Ribeiro, J. Órfão, J.J.M. Órfão, M.F.R. Pereira, Hydrolytic hydrogenation of cellulose to ethylene glycol over CNT supported Ru-W bimetallic catalysts, Cellulose 25 (2018) 2259–2272.
[37] Y. Yang, W. Zhang, F. Yang, D.E. Brown, Y. Ren, S. Lee, D. Zeng, Q. Gao, X. Zhang, Versatile nickel-tungsten bimetallics/carbon nanofiber catalysts for direct conversion of cellulose to ethylene glycol, Green Chem. 18 (2016) 3949–3955.
[38] L.S. Ribeiro, J.J.M. Órfão, M.F.R. Pereira, Direct catalytic conversion of agro-forestry biomass wastes into ethylene glycol over CNT supported Ru and W catalysts, Ind. Crop. Prod. 166 (2021), 113461.
[39] K. Fabičovicová, O. Malter, M. Lucas, P. Claus, Hydrogenolysis of cellulose to valuable chemicals over activated carbon supported mono- and bimetallic nickel/tungsten catalysts, Green Chem. 16 (2014) 3580–3588.
[40] G. Liang, H. Cheng, W. Li, L. He, Y. Yu, F. Zhao, Selective conversion of microcrystalline cellulose into hexitols on nickel particles encapsulated within ZSM-5 zeolite, Green Chem. 14 (2012) 2146–2149.
[41] I.G. Baek, S.J. You, E.D. Park, Direct conversion of cellulose into polyols over Ni/W/SiO2-Al2O3, Bioresour. Technol. 114 (2012) 684–690.
[42] Y. Cao, J. Wang, M. Kang, Y. Zhu, Efficient synthesis of ethylene glycol from cellulose over Ni–WO3/SBA-15 catalysts, J. Mol. Catal. Chem. 381 (2014) 46–53.
[43] L.S. Ribeiro, J.J.M. Órfão, M.F.R. Pereira, Enhanced direct production of sorbitol by cellulose ball-milling, Green Chem. 17 (2015) 2973–2980.
[44] Q. Wei, X. Chen, Y. He, J. Fu, J. Liang, X. Wei, L. Wang, Ni Nanoparticles supported on N-doped carbon nanotubes for efficient hydrogenation of C5 hydrocarbon resins under mild conditions, Microporous Mesoporous Mater. 333 (2022), 111727.
[45] J. Pang, M. Zheng, A. Wang, T. Zhang, Catalytic hydrogenation of corn stalk to ethylene glycol and 1,2-propylene glycol, Ind. Eng. Chem. Res. 50 (2011) 6601–6608.
[46] J. Pang, M. Zheng, R. Sun, L. Song, A. Wang, X. Wang, T. Zhang, Catalytic conversion of cellulosic biomass to ethylene glycol: effects of inorganic impurities in biomass, Bioresour. Technol. 175 (2015) 424–429.
[47] C. Li, M. Zheng, A. Wang, T. Zhang, One-pot catalytic hydrocracking of raw woody biomass into chemicals over supported carbide catalysts: simultaneous conversion of cellulose, hemicellulose and lignin, Energy Environ. Sci. 5 (2012) 6383–6390.